

## Measurement Note

# A stiff facility for controlled pre-cracking in fracture toughness tests

### Abstract

The issue of compliance in controlled cracking of fracture toughness test-pieces is discussed with particular regard to hard and stiff material made by powder routes, including ceramic, hardmetals and hard powder metallurgy materials.

The design and functionality of a stiff mechanical device for pre-cracking fracture toughness test-pieces is described. It operates on the basis of a stiff frame with a piezoelectric load cell and a stepper motor driven wedge to provide displacement, and a frame and load cell combined compliance of about  $2 \mu\text{m/kN}$  at 5 kN force has been achieved.

Preliminary experiments with the facility reveal a number of issues associated with increased compliance at lower applied forces, much of which is associated with compliance of the flexural loading jig used within the test machine, particularly the localised contacts between rollers and jig parts.

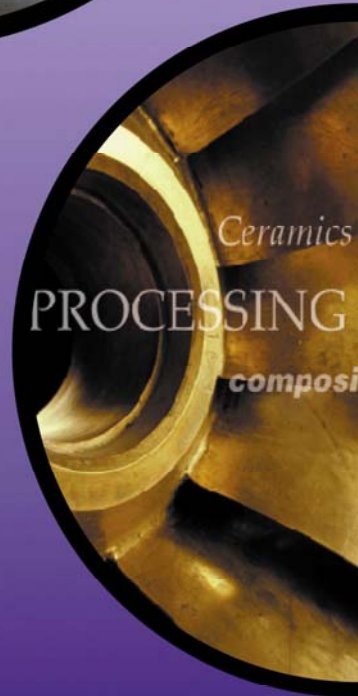
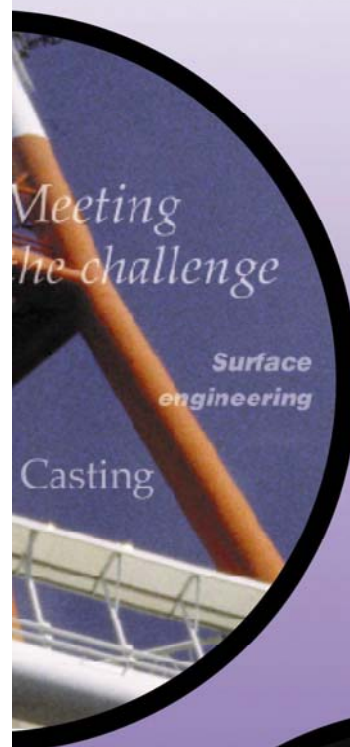
Controlled fracture has been achieved in two alumina ceramics and in a PM tool steel which displayed discontinuous fracture. Controlled fracture in hardmetals has not yet been achieved, and requires further experiments with improved chevron notch designs.

**R Morrell and M Parfitt**

**Division of Engineering and Process Control**

**November 2005**

**ISSN 1744-3911**



## 1. INTRODUCTION

The measurement of fracture toughness of relatively hard brittle materials (ceramics, hardmetals, tool steels, etc.) is something of a challenge, especially in small test-pieces. It is generally accepted that valid toughness data can be obtained only from a crack running under controlled propagation, and this is difficult to achieve unless the test-piece is pre-cracked. Attempts to do this from a machined notch in a flexural test bar typically result in uncontrolled fracture, and to an overestimate of toughness because crack initiation is generally more difficult than its propagation. The machining processes to insert a notch, while initiating microcrack damage, do not produce the equivalent of a sharp crack, since the cutting damage needs to 'join up' before propagation can occur. The residual stresses put into the material by cutting the notch, which are usually compressive in nature, make matters worse.

The generation of sharp cracks usually requires careful experimentation. Some examples are as follows:

**Single-edge pre-cracked beam method (1):** Starting from a straight-through sawn notch, in the bridge method the test-piece is placed on two rigid supports separated by a gap of typically 10 mm, with the notch midway between the supports. A pusher plate is placed on top, and loaded by a test machine. The constraining stress field permits a crack to 'pop in' and stop. The main difficulties are designing a bridge jig of appropriate compliance and adjustability, obtaining alignment, and producing straight-through rather than angled pre-cracks. In skilled hands, the method works well for materials of toughness up to about  $10 \text{ MPa m}^{1/2}$ . Alternative methods include axial compressive loading combined with flexural impact, such as has been reported for tool steels (2).

**Indentation pre-cracking:** Placing a Vickers or Knoop indentation in a ceramic flexural test-piece can produce radial cracking from the indentation corners. By removing the

indentation damage (typically 3-4 times the indentation depth) to avoid the effects of unknown residual stresses, the test-piece should have effectively a stress-free semi-elliptical pre-crack. The size of the pre-crack is measured after fracture using fractography. The technique works for fine-grained materials of toughness less than about  $5 \text{ MPa m}^{1/2}$ , but fractography becomes unreliable for coarser-grained materials, and for tougher materials which do not form complete half-penny cracks under indentation.

**Chevron notch pre-cracking:** By placing a sharp-tipped chevron notch into a flexural test-piece of all types of hard material it is possible to combine pre-cracking with fracture toughness measurement provided that controlled initiation and growth of the crack occurs from the chevron tip. This is the key issue. Generally, a conventional testing machine has too much compliance, to the extent that as the crack propagates and the force drops, the machine relaxation drives the crack and produces unstable crack growth. A stiff machine is required for many materials. In addition, machining the notch introduces compressive residual stresses, and these tend to make the initial crack 'pop-in' uncontrolled.

Although the above methods can be made to work for the majority of advanced technical ceramics, they do not work adequately or validly for tougher hardmetals and PM tool steels. The target of the current research is to identify whether the development of a very stiff mechanical system can aid the generation of controlled pre-cracks and de-skill the process.

## 2. STIFF PRE-CRACKING FACILITY

### 2.1 Stiffness

In a test facility, the control of crack growth depends on ensuring that the energy input by the test machine is less than or equal to the energy required to create new surface area. In mathematical terms [3]:

$$G(u, a) = G_{system}(u, a) + \int_0^A R(a) dA \quad (1)$$

$$= \frac{u^2}{2C(a)} + B \int_0^a R(a) da = \frac{u^2}{2C(a)} + Ba \frac{K_{Ic}^2}{E'}$$

where  $G$  is the total Gibbs free energy,  $G_{system}$  is the Gibbs free energy of the mechanical part of the system displaced a distance  $u$ ,  $A$  is the crack area,  $B$  is the test-piece width, and  $C(a)$  is the system mechanical compliance.  $R(a)$  is the surface energy of the crack of length  $a$  in the test-piece, related to the fracture toughness,  $K_{Ic}$  and plane strain elastic modulus  $E' = E(1-\nu)$ . The system compliance comprises the compliance of the test-piece in flexure,  $C_S(a)$  and the compliance of the test jig and loading frame  $C_M$ , including all the roller contacts with the test-piece, i.e.:

$$C(a) = C_S(a) + C_M \quad (2)$$

$C_S(a)$  can be computed from compliance relationships in the computation of fracture toughness (see below). Stable crack growth can occur when [4]:

$$\left[ \frac{\partial G}{\partial a} \right]_u < \left[ \frac{\partial G_c}{\partial a} \right] \quad (3)$$

where  $G_c$  is the fracture toughness. Assuming no R-curve behaviour,

$$\frac{\partial G_c}{\partial a} = 0 \quad (4)$$

and hence the condition for stability becomes

$$\left[ \frac{\partial G}{\partial a} \right]_u < 0 \quad (5)$$

Evaluation of the above equations for specific test-piece geometries and machine compliance can be used to show that a crack must already have a certain length, which increases with increasing machine compliance relative to test-piece compliance, to achieve stable growth [3]. However, it is difficult to predict what the stiffness requirement for popping in pre-cracks is. The above analysis route demonstrates that the total load train compliance should be small compared with the compliance of the test-piece itself,

preferably of the order one-fifth or one-tenth of that of the test-piece, such that there is minimal driving energy from the machine once the crack starts to grow. The roller contacts in the four-point bending jig, as well as all other contacts in the load train, will contribute to machine compliance in a load and modulus dependent way. In addition, while the overall design concept needs to optimise the frame, drive and load-cell stiffness, it is difficult to predict how stiff a design will be, especially in the lower force range up to 1 kN. Load train stiffness depends primarily on the execution of engineering.

## 2.2 Design concept

A conventional mechanical testing machine has numerous compliant elements, including the load cell, the jiggling arrangements, the ram or lead-screw system, and the main frame. In order to reduce the compliance, attention needs to be paid to all these elements, preferably removing some of them altogether. The principal target constraining the design of the system is the force range. In the present case, the initial intention was to provide for wide dimensional flexibility a force capability up to 50 kN with as much as 2 - 3 mm of displacement, and this ruled out the use of a piezo-actuator, as used in references [3] and [5], as the means of providing stiff motion control. It was decided to employ a design involving a wedge-driven pre-loaded ram inside a stiff frame, with a stiff piezo load cell to measure the force applied to the test-piece (Figure 1).

The ram/wedge contact is preloaded to approximately 50 kN in its mid position by a pair of disc springs in order to remove slack between the ram, the wedge surfaces and the frame. The wedge surfaces are coated with a diamond-like carbon (DLC) coating to reduce friction. The wedge is driven by a linear actuator comprising a non-rotating lead screw on which an internally threaded gear sits. This gear is driven by a worm, in turn driven by a stepper motor operating through a gear box. The speed range is adjusted electronically to give fixed nominal ram displacement rates in

the range 0.26 to 13.7  $\mu\text{m/s}$ . Speed calibration was performed using an independently calibrated displacement transducer set within a steel pillar placed on the load cell and contacting the upper part of the frame.

Unfortunately this arrangement has led to some backlash in the drive system on reversing, which may be removable by additionally pre-loading the wedge.

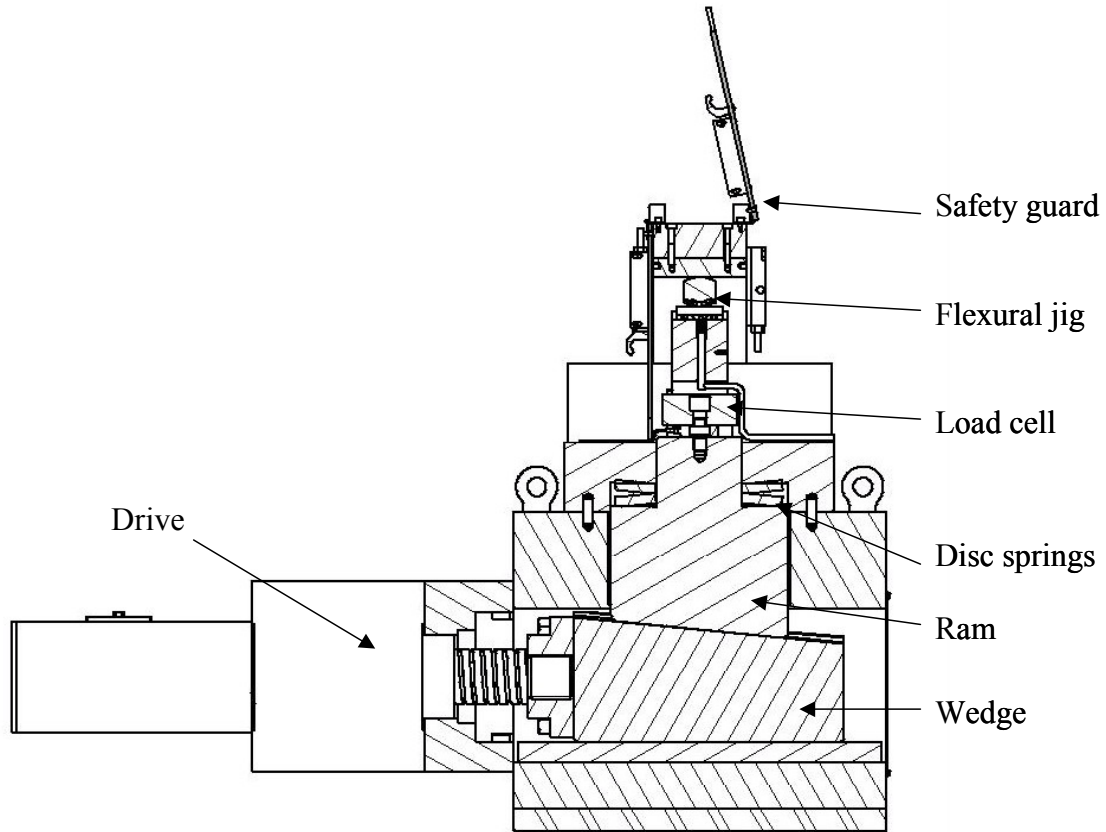


*Figure 1: Cross-section of stiff pre-cracking apparatus*

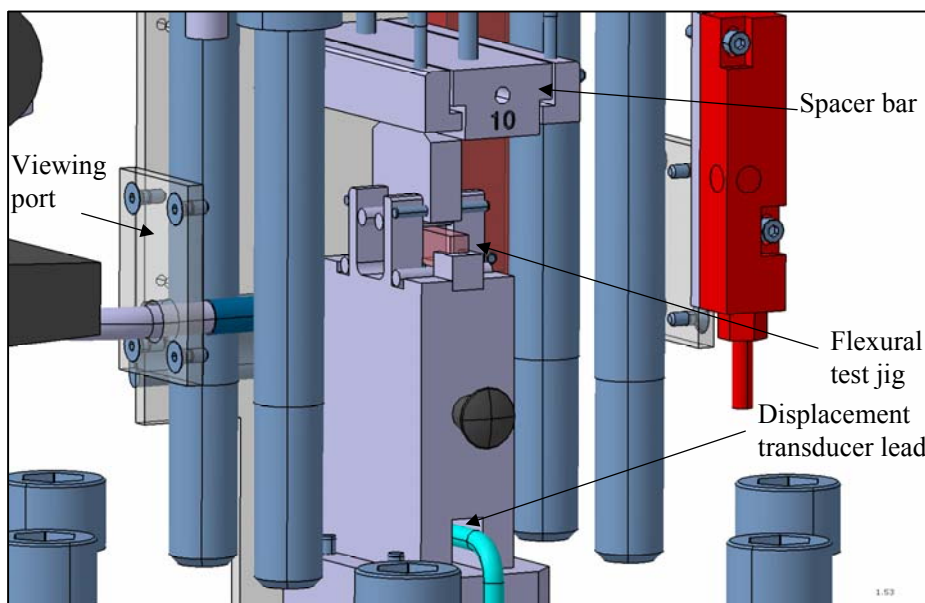


*Figure 2: Detail of flexural test jig inside system with frame removed.*

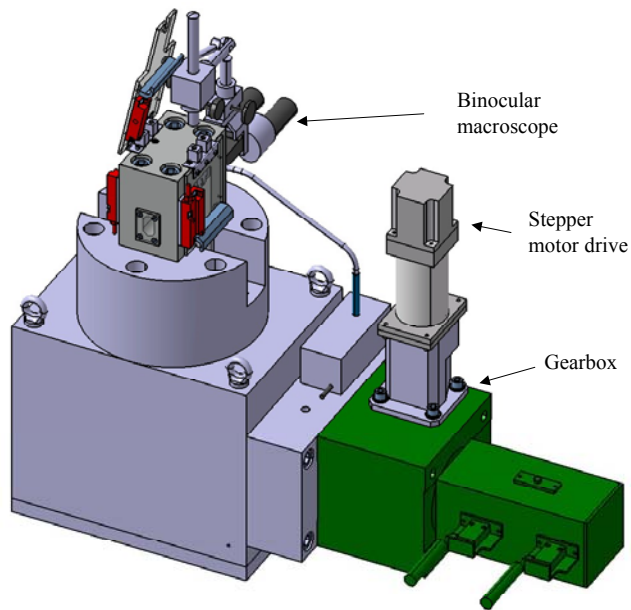


**Figure 3:** Rear view of complete unit.

The removable four-point flexural test jig sits on a platform on top of the load cell, which itself is bolted directly to the top of the ram. The system is design geometrically to accept a range of different test-piece heights from 3 mm to 10 mm by using an appropriate thickness spacer bar (Figure 2). The jig is semi-articulating, intended for machined test-pieces, rather than fully articulating, in order to reduce compliance, and employs 5 mm diameter tungsten carbide rollers operating with a 30mm outer span and 10 mm inner span. A displacement transducer is located within the lower jig unit contacting the underside of the test-piece to one side of a central notch. On an unnotched bar, it has been calculated that the transducer should record a flexural displacement approximately 10% more than the displacement opposite the loading rollers. A Labview program was written to log force, displacement and time data.

### 2.3 Compliance determination

Load frame compliance can be determined by replacing the flexural jig with a steel pillar and loading directly. The compliance can be computed from the force and the nominal machine displacement based on speed and time. Figure 4 shows that after being idle for some time, the machine is soft during the first

loading cycle, but stiffer and repeatable during subsequent cycles. The compliance was determined to be 7.08, 4.09 and 1.99  $\mu\text{m}/\text{kN}$  at 0.5, 1.0 and 5.0 kN respectively. By comparison, the anticipated compliance of the compressed pillar is only 0.27  $\mu\text{m}/\text{kN}$  assuming a Young's modulus value of 200 GPa.

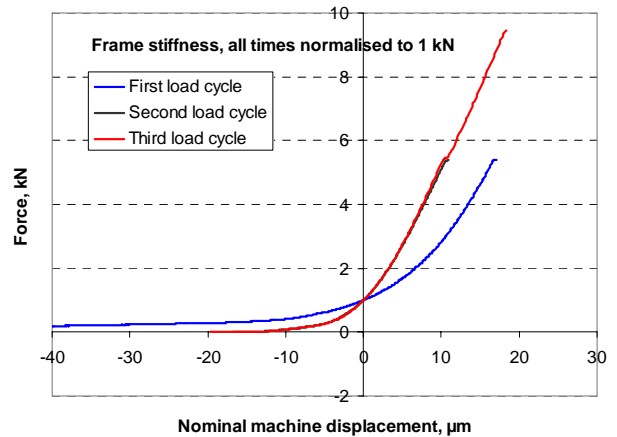


**Figure 4:** The loading parts of three consecutive load cycles using a steel pillar to obtain frame compliance, showing good repeatability between second and third cycles.

An estimate of the test-jig compliance can be obtained by inserting a large bar, e.g. a steel tool, into the jig and performing similar loading cycles. The results of the tests are shown in Table 1, which lists the machine compliance from the ram displacement/force data, the apparent test-piece compliance from the displacement transducer, and the computed test-piece compliance assuming a Young's modulus value of 200 GPa. The total compliance is rather larger than the values for the ram and frame determined above, and originate from the test jig which contains a number of localised contacts. An attempt was made to remove two pairs of contacts by using rollers with a single flat, which was placed in contact with the flat jig parts to remove most of the Hertzian indentation on the test jig parts<sup>1</sup>. The effect

<sup>1</sup> It was recognised that if these flattened rollers were used for testing this would remove their ability to roll as the test-piece deflects, and thus could introduce frictional drag and introduce an error in testing.

(data in parentheses in the Table) was only a small reduction, suggesting that an individual WC roller on steel jig contact had a compliance of about 0.24  $\mu\text{m/kN}$ . Replacing the top steel loading block with a stiffer alumina ceramic block reduced the total compliance by 6.4  $\mu\text{m/kN}$ , a result which suggests that modifications need to be made to the flexural jig to reduce its compliance, and plans have been laid to replace various parts currently made in steel with a WC

hardmetal of approximately three times the modulus. The difference between the computed flexural compliance of the test-piece and the directly measured value has to be ascribed to indentation of the test-piece and the test jig base by the rollers under the applied force. Again, modifications are needed to reduce this difference, but there will always be an issue with test-piece roller indentation.

**Table 1: Compliance calibration using a 9.4 mm x 9.4 mm steel bar in the flexural jig (data in parenthesis obtained after replacing round rollers with flatted rollers)**

Force level, kN	Total compliance from machine displacement, $\mu\text{m/kN}$	Apparent compliance of steel tool test-piece, $\mu\text{m/kN}$	Computed test-piece flexural compliance, $\mu\text{m/kN}$
0.5	19.6 (18.1)	7.20 (7.70)	3.56
1	16.8 (15.6)	6.65 (6.43)	
3	12.2 (11.8)	6.32 (6.12)	

### 3. PRE-CRACKING OF NOTCHED BEAMS

#### 3.1 Theory

The compliance of a rectangular section unnotched beam in four-point bending is given by [6]:

$$C = \frac{\delta}{F} = \frac{2d_1^2}{E'BW^2} \left[ \frac{2(d_1 + 3d_2)}{W} + \frac{W(1-\nu)}{(d_1 + d_2)} \right] \quad (5)$$

between the pairs of loading points, where  $\delta$  is the load-point deflection,  $F$  is the applied force,  $E'$  is the plane strain value for Young's modulus =  $E/(1 - \nu^2)$ ,  $B$  is the width,  $W$  is the depth in the direction of flexure,  $d_1$  is the distance between adjacent inner and outer rollers, and  $d_2$  is the half-span of the inner rollers. The first term in brackets is for a thin beam, and the second is a wedging correction. Using the 30 mm/10 mm span four point bending geometry, a WC hardmetal test-piece with  $B = 3$  mm and  $W = 5$  mm and  $E = 600$  GPa will have thus a load-point compliance of about 22.2  $\mu\text{m/kN}$ . Experimentally a value of 26.5  $\mu\text{m/kN}$  was obtained, a difference which

is in line with the results shown in Table 1 for a steel beam, and results from residual jig compliance.

When a straight-through notch is placed in the centre of the beam, the situation becomes more complicated. The relationship taken from fracture mechanics analysis has to be used [1, 6, 7]:

$$\frac{\partial C}{\partial \alpha} = \frac{2Y^2}{EB} \quad \text{where } Y = \left( \frac{2d_1}{W} \right) \frac{3\Gamma\sqrt{\alpha}}{2(1-\alpha)^{3/2}} \quad \text{and}$$

$$\Gamma = 1.9887 - 1.326\alpha$$

$$\frac{(3.49 - 0.68\alpha + 1.35\alpha^2)\alpha(1-\alpha)}{(1+\alpha)^2} \quad (6)$$

where  $\alpha = a/W$  where  $a$  is the notch depth. It should be noted that  $\Gamma$  (given above for pure bending) is a function of  $d_1$  and  $d_2$ . A numerical integration has to be performed to obtain  $C$ . Figure 5 shows the trend for a hardmetal test-piece. It can be seen that in order to ensure that the test-piece has a much larger compliance than the machine, and thus dominate the cracking process,  $a/W$  must typically be greater than 0.5, preferably more

than 0.7. There are therefore likely to be intrinsic difficulties in initiating non-catastrophic fracture in such a material. For a PM tool steel, the modulus is about one-third of that of WC, so a similar-sized test-piece offers more prospect for success.

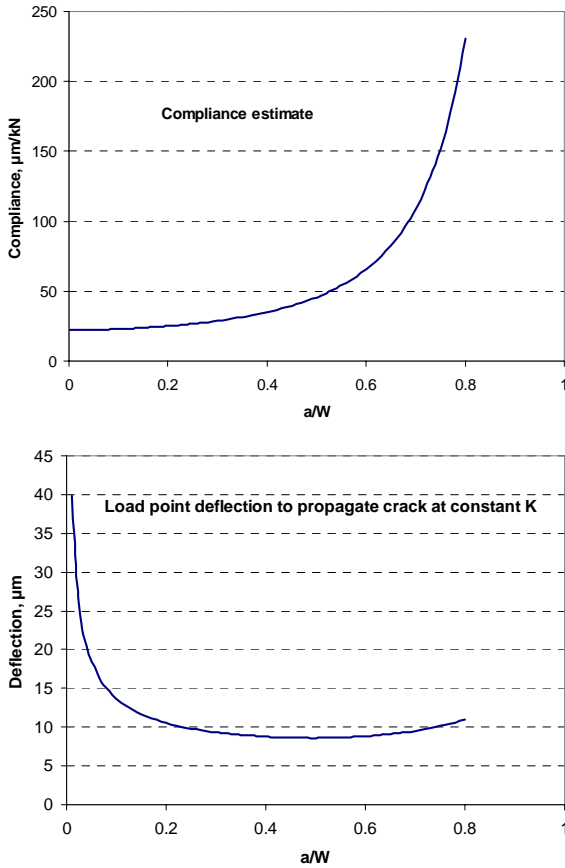


**Figure 5:** Computed load-point compliance and deflection to cause a straight-through crack to run in a WC hardmetal test-piece with:  $E = 600 \text{ GPa}$ ,  $B = 3 \text{ mm}$ ,  $W = 5 \text{ mm}$ ,  $d_1 = 10 \text{ mm}$ ,  $d_2 = 5 \text{ mm}$ , and  $K_{Ic} = 10 \text{ MPa m}^{1/2}$ .

For stiff/strong materials with minimal initiating damage at the root of the notch, prospects are likely to be better for crack initiation from a chevron notch [2]. The stress concentration at the notch tip permits easier initiation. In this case, as the crack propagates down the chevron, the crack line width increases. There is a maximum in the driving force required, which is related to the shape of the chevron, corresponding to a minimum in the value of  $Y$ ,  $Y_{min}^*$ . In this case  $Y^*$  is also a function of the chevron angle. No simple general analytical expression exists, but the

Bluhm slice model [8] is commonly used to compute compliance. Explicit expressions appear in ASTM C1421 [9] for fracture toughness of particular geometries, while a more flexible but less accurate approximation for fracture toughness is given by Munz and Fett [10]:

$$K_{I, cnb} = Y_{min}^* \left[ \frac{2P_{max}d_1}{BW^{3/2}} \right] \text{ where}$$

$$Y_{min}^* = (3.08 + 5.00\alpha_0 + 8.33\alpha_0^2) \times$$

$$\left( 1 + 0.007 \left( \frac{4d_2(d_1 + d_2)}{W^2} \right)^{1/2} \right) \left( \frac{\alpha_1 - \alpha_0}{1 - \alpha_0} \right)$$

where  $\alpha_0 = a_0/W$  is the fractional depth of the chevron tip, and  $\alpha_1$  is the fractional depth of the chevron run-out in the side walls.

## 3.2 Experiment

### 3.2.1 Ceramics

Initial experiments with asymmetrically notched 88% alumina ceramic test-pieces from previous work [11] with  $\alpha_0 \sim 0.4$  showed that controlled fracture could be readily obtained. Figure 6 shows an example with a clear maximum in the applied force occurred permitting  $K_{I, cnb}$  to be determined ( $3.48 \text{ MPa m}^{1/2}$  using the above equations).

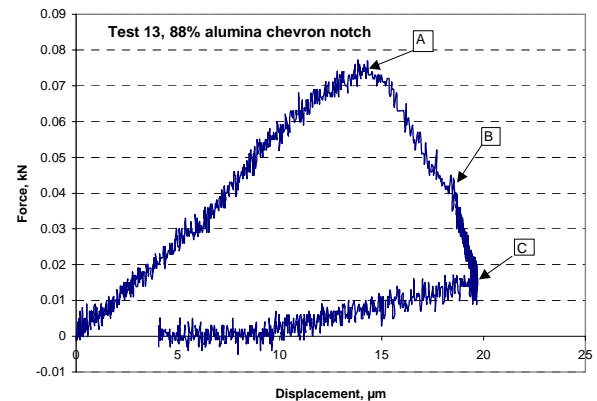


**Figure 6:** Fracture toughness determination of chevron notched test-piece of 88% alumina loaded at  $0.26 \mu\text{m/s}$  ram displacement rate, showing non-linearity in loading above  $0.055 \text{ kN}$ , rising to a peak at A. The ram movement was stopped at B, but controlled subcritical crack propagation continued until C when the test-piece was unloaded.

A second series of experiments was performed on the same material but using straight-through vee-notches produced by the razor-blade honing technique. The depth of the vee-notches gave  $\alpha_0$  values in the range 0.23 to 0.30. Measurements of test-piece compliance taken from the steepest part of the force/displacement corrected for machine and test jig compliance and for the location of the transducer tip relative to the loading roller are compared with computed compliance in Figure 7, showing reasonable agreement. An example of a complete test is shown in Figure 8. It is clear that subcritical crack growth is occurring before a rapid load drop, although this load drop is not catastrophic, and stops at an  $\alpha$  value of 0.88. Taking the maximum force applied and the original vee-notch depth, fracture toughness values obtained were  $3.5 \pm 0.5 \text{ MPa m}^{1/2}$ , a value in good agreement with the chevron notch tests. In practice, the subcritical crack growth to this point underestimates the true crack length. If compliance can be used as a measure of crack length, in principle the toughness can be computed for all crack lengths, but in the present case, applying this concept leads to a rather higher toughness values than the above figures. Unfortunately, it has been determined that the current design of the jig, specifically, the location of the test-piece transducer, makes accurate compliance estimation for notched or cracked test-pieces impossible to obtain (note that while the curvature of a straight beam, and hence the deflection at any point, can be computed, that of a notched beam cannot readily be performed). It would be necessary to re-design the transducer location such that the measured deflection corresponded with that assumed for the basis of the compliance calibration.

Nonetheless, it is clear that although the facility is operating at its lower limits particularly of its force resolution, it has been shown to be sufficiently stiff to be capable of subcritically pre-cracking vee-notched beam test-pieces.

### 3.2.2 PM tools steels

Using a facility at the University of Bradford, test-pieces with  $W \sim 9.55 \text{ mm}$ ,  $B \sim 2.84 \text{ mm}$  and containing a  $90^\circ$  angle (*i.e.* short length) chevron notch with  $\alpha_0 \sim 0.09$  and  $\alpha_1 \sim 0.23$  had been successfully pre-cracked using a flexural impact rig in which the test-piece is pre-compressed to halt the growing crack [2].

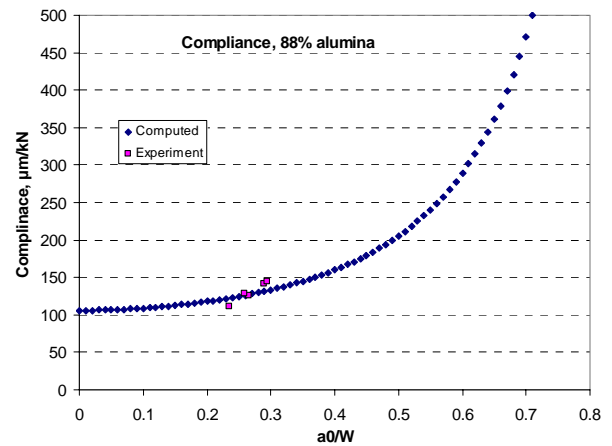


**Figure 7:** Experimental compliance for 88% alumina vee-notched test-pieces compared with computed values, assuming a Young's modulus of 260 GPa.

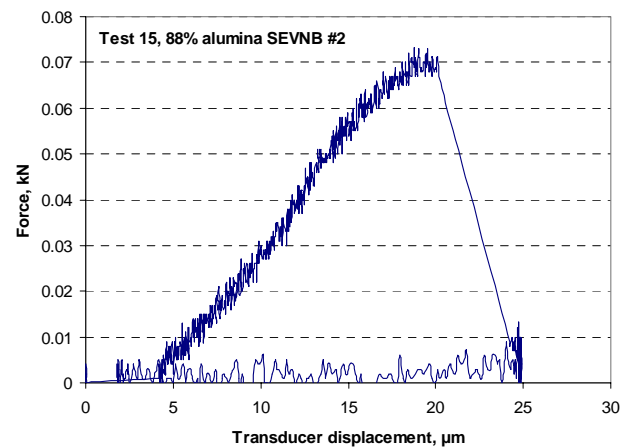


**Figure 8:** Force/displacement curve for 88% alumina vee-notched beam test-piece showing clear peak before rapid, but not catastrophic crack growth.

The first test in the present stiff facility employed one of these test-pieces, but controlled crack pop-in and growth did not occur. It was judged that the compliance of the test-piece was similar to that of the test

facility. To increase the starting compliance, a series of three test-pieces were prepared in which the notch was machined to a sharper chevron (about  $60^\circ$ ) with progressively greater  $\alpha_0$  and  $\alpha_1$  values. In conducting tests on these test-pieces it was found that a threshold existed for obtaining controlled growth at  $\alpha_0 \sim 0.3$ , at which the compliance was greater than  $35 \mu\text{m}/\text{kN}$ . Two examples are shown in Figure 9. Most noteworthy was the finding that the crack propagation was not smooth, but proceeded in a series of jumps following elastic loading which could be viewed directly on the side of the test-piece. Detail of the behaviour of one of these tests is shown in Figure 10.

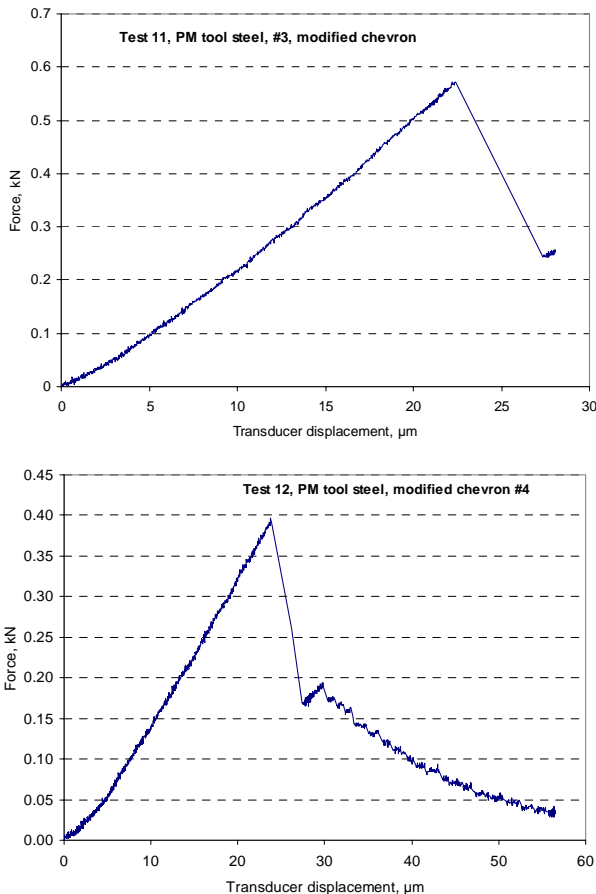


**Figure 9:** Force/transducer deflection trace for PM tool steel test-pieces (upper) with  $\alpha_0 \sim 0.35$  and  $\alpha_1 \sim 0.78$ , showing non-catastrophic pop-in, and (lower) with  $\alpha_0 \sim 0.48$  and  $\alpha_1 \sim 0.88$ , showing non-catastrophic pop-in and a series subsequent crack jumps with increasing deflection.

Fracture toughness values were taken from the first load peak or hold after pop-in, and values of approximately  $10 \text{ MPa m}^{1/2}$  were obtained using the chevron notch analysis. However, strictly, the standard analysis is inappropriate because it assumes a monotonic  $Y^*$  function, and not a series of unstable jumps. Observation of the fracture surfaces reveals no obvious steps in the propagation of the crack, and no evidence of prior particle boundaries controlling the fracture (Figure 10).

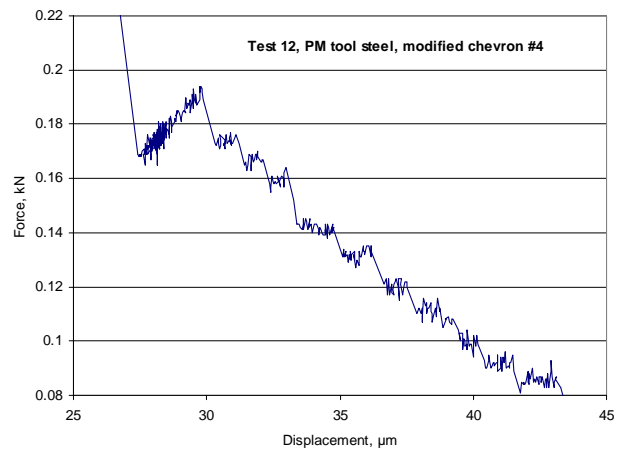


**Figure 10:** Detail of the force/transducer displacement curve showing the effect of crack-front movement in a series of steps following progressive flexure of the test-piece.

It can be concluded that although the PM material used in this trial showed abnormal behaviour, controlled crack growth can be obtained provided that the chevron is deep enough.

### 3.2.3 Hardmetals

Hardmetals pose the greatest challenge to pre-cracking because their high elastic modulus leads to low compliance, and the stiffness of the test machine becomes paramount. At present, the instrument has not achieved controlled initiation on a 9% Co hardmetal, either on a  $90^\circ$  notched specimen, or on a straight-through notch  $\alpha_0 \sim 0.32$  produced by electrodischarge machining (EDM), even when loaded in parallel with an unnotched test-piece. This indicated that not only does

the test jig stiffness needs to be improved, but that the starting notch depth needs to be greater. Future trials will include deeper chevron notches introduced by EDM.

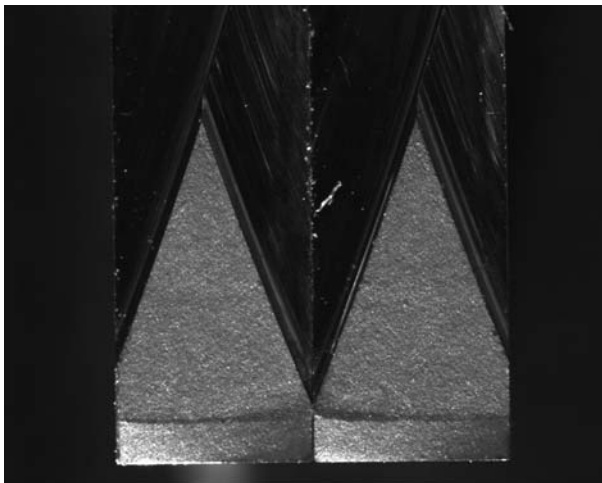
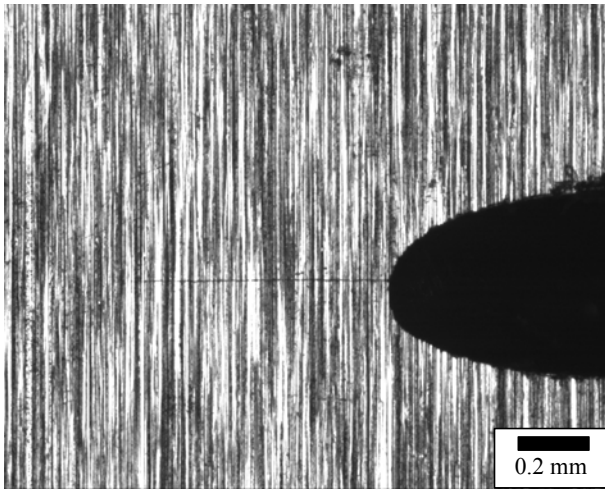


**Figure 10:** *Controlled cracks in PM tool steel (upper) crack running out of the chevron region, (lower) fracture surface showing no significant features over the chevron region (the step at the lower side was due to manual final fracture of the test-piece).*

#### 4. DISCUSSION

The concept of controlled crack development and growth relies on ensuring that the energy required for an increment in crack length is greater than the driving energy available in the test-piece itself and in the machine. In the main, once a crack has been initiated, the facility in its present design can produce controlled growth, but the area of concern remains the difficulty with crack pop-in. It is

clear that the four-point flexural jig needs to be stiffened further to enable pop-in from chevron notches in hardmetals to be achieved. The facility successfully employed for hardmetals described in [12] appears [13] to have about one-half of the compliance achieved so far in the present facility.

#### 5. CONCLUSIONS

The development of a facility sufficiently stiff to minimise the elastic driving energy in crack development and growth experiments on hard relatively brittle materials has been described. A frame compliance as low as  $2 \mu\text{m/kN}$  at 5 kN force has been achieved, but it is more compliant at lower forces. It has been established that the flexural testing facility is not as stiff as ideally needed for testing all types of brittle materials. Nonetheless, it has operated successfully on both chevron and straight-through vee-notched ceramic materials, and on a PM tool steel which displayed discontinuous fracture behaviour. It has not as yet been successful with hardmetals, but the solution may lie in modified test-pieces, and redesign of the flexural jig to reduce compliance further.

#### ACKNOWLEDGEMENTS

This work has been performed as part of Department of Trade and Industry's Materials Metrology Programme 2002-5.

#### References

- [1] Nose, T., Fujii, T., "Evaluation of fracture toughness for ceramic materials by a single-edge-pre-cracked-beam method", *J. Amer. Ceram. Soc.*, 1988, **71**(5), 328-33.
- [2] Wronski, A.S., Rebbeck, M.M., Amen, S.A., "Fracture mechanisms and mechanics of an 18-4-1 high speed steel", *J. Mater. Sci.*, 1988, **23**, 2213-9.
- [3] Takagi, S, Nakano, H., Sakai, M., "Development of a testing machine for three-point bending of ceramics in

- controlled crack extension”, *Bull Nat. Res/ Inst. Metrology (Japan)*, 1998 **47**(4) 343-6.
- [4] Sigl, L.S., “On the stability of cracks in flexure specimens”, *Int. J. Fracture*, 1991, **51**, 241-54.
- [5] EXAKT Vertriebs GmbH brochure, [http://www.exakt.de/en/st\\_system.htm](http://www.exakt.de/en/st_system.htm)
- [6] Munz, D, Bubsey, R.T., Shannon, J.L., “Fracture toughness determination of Al<sub>2</sub>O<sub>3</sub> using four-point bend specimens with straight-through and chevron notches”, *J.Amer. Ceram. Soc.*, 1980, **63**(5-6), 300-305.
- [7] Srawley, J.E., Gross, B., *ASTM Spec. Tech. Publ. No. 601*, 1976, pp559-579.
- [8] Bluhm, J.I. ‘Slice synthesis of a three-dimensional work of fracture specimen’, *Eng. Fract. Mech.*, 1975, **7**, 593-604.
- [9] ASTM C1421 Standard test methods for determination of fracture toughness of advanced ceramics at ambient temperature.
- [10] Munz, D., Fett, T., in *Werkstoff-Forschung und -Technik 8, Mechanisches Verhalten Keramischer Werkstoffe*, Springer Verlag, Berlin, 1989, p33.
- [11] Paddon, J.M., Morrell, R., "Evaluation of the chevron notch fracture toughness test for brittle materials", NPL Report DMM (A) 72, July 1992.
- [12] Garber, E., Schleinkofer, U, Greif, G., “A new approach for precracking fracture toughness specimens of hardmetals”, *Proc. 16th Int. Plansee Seminar*, 2005, paper HM90, 1183-96.
- [13] Garber, E., private communication, November 2005.

